Available online at www.sciencedirect.com
ScienceDirect
Tetrahedron
Tetrahedron 63 (2007) 3168–3172

# Brightly full-color emissions of oligo(*p*-phenylenevinylene)s: substituent effects on photophysical properties

Tonggang Jiu,[a,b] Yuliang Li,[a,*] Huibiao Liu,[a] Jianping Ye,[c] Xiaofeng Liu,[a,b] Li Jiang,[a] Mingjian Yuan,[a,b] Junbo Li,[a,b] Cuihong Li,[a,b] Shu Wang[a] and Daoben Zhu[a,*]

[a]*Beijing National Laboratory for Molecular Sciences (BNLMS), CAS Key Laboratory of Organic Solids, Institute of Chemistry, Chinese Academy of Sciences, Beijing 100080, PR China*
[b]*Graduate School of Chinese Academy of Sciences, Chinese Academy of Sciences, Beijing 100080, PR China*
[c]*Key Laboratory of Photochemistry, Institute of Chemistry, Chinese Academy of Sciences, Beijing 100080, PR China*

Received 9 December 2006; revised 2 February 2007; accepted 5 February 2007
Available online 8 February 2007

**Abstract**—A simple and effective strategy for synthesis of bis-dipolar trimeric OPVs (a–g) with same push–pull electron groups at the two ends is presented. Their photophysical and electrochemical properties were investigated by UV–vis, fluorescence spectroscopies, and voltammetry techniques. A successful tuning in the emission color was achieved and the LUMO energy level was found to correlate with the Hammett constant of the respective substituents, providing a powerful strategy for prediction of the photoelectrical properties of the new chromophores.


## 1. Introduction

Molecular semiconducting materials have been extensively investigated for various technological functional properties for next-generation electronic and optoelectronic applications, such as electroluminescent devices,[1–4] field-effect transistors,[5] photovoltaic devices,[6] electro-optic modulators, and solid-state lasers[7] in the past decade. In addition to polymeric materials, functionalized π-conjugated oligomers have recently received considerable attention due to their unique and interesting optoelectronic properties and the need for vacuum deposition processes.[8] A trend that has recently emerged in this field is the so-called 'oligomer approach',[9–11] in which low and intermediate molecular weight organic molecules with high luminescence quantum yields were synthesized to serve as the active layers in optoelectronic devices such as organic light-emitting diodes (OLEDs) and lasers. Among these functional oligomers, oligo(*p*-phenylenevinylene)s (OPVs) were of particular interest because of their stability, high luminescent efficiency, and ease of synthesis.[12,13] Recently Meijer and co-workers reported that chiral oligo(*p*-phenylenevinylene) (OPV) molecules self-assembled to form helical stacking structures in solution.[14] In addition, they reported that structural order in the self-assembled helix significantly affects the efficiency of energy transfer between OPVs.[15] Stupp and co-workers investigated the use of self-assembling molecules to create highly ordered and nanostructured films based on OPV and silicate in one step.[16] OPV was therefore an interesting target for both organic light-emitting diodes (OLEDs) and organic solar cells.

The development of full-color emitting devices is one of the main challenges in optical displays.[17,18] Small molecules are considered as the candidates due to their extremely high fluorescence quantum efficiencies in the visible spectrum and ease of processing. So far, the major obstacle in the fabrication of OLED-based full-color displays is the limited availability of conjugated oligomers that span the whole visible spectrum, while possessing similar emissive characteristics, physical properties, and processability. In this regard, it would be interesting and meaningful to develop new luminescent oligomers with intrinsically electronic structures for the development of highly efficient and stable OLEDs. To this goal, the key is to develop a synthetic methodology to effectively adjust and control the HOMO and LUMO levels of conjugated oligomers. Chemical modification can often adjust the band gap of light-emitting oligomers, which leads to effective color tuning. Herein, we reported the synthesis and characterization of a series of novel well-defined OPV trimers consisting of two symmetrical electron-withdrawing (EWG) or electron-donating groups (EDG) attached to the end aromatic ring to adjust the HOMO and LUMO levels of the resulting oligomers. The two symmetrically medial-substituted hydrophobic alkoxy chains were used to improve the solubility of the trimers.

*Keywords*: Oligomer; Hammett substituent; Substituent effect; Full color.
* Corresponding authors. Tel.: +86 10 62588934; fax: +86 10 82616576 (Y.L.); e-mail: ylli@iccas.ac.cn

0040–4020/$ - see front matter © 2007 Elsevier Ltd. All rights reserved.
doi:10.1016/j.tet.2007.02.012

## 2. Results and discussion

### 2.1. Synthesis and photophysical property

The synthesis of bis-dipolar trimeric OPVs (a–g) modified by alkoxy group in the center aromatic ring and by same push–pull electron groups at the two ends was effectively accomplished by Wittig–Honor reaction as shown in Figure 1 and described in detail in Section 4.

The photoluminescence and UV–vis absorption spectra of the OPVs recorded at room temperature in chloroform solution are shown in Figure 1 (and SFig. 1 in Supplementary data). The optical transitions of the OPVs shift to longer wavelengths with increasing electron-withdrawing abilities of end-substituent R. In regard to structure–optical property relationship, it was found that the relativity for substituent effect on absorption spectra, excitation spectra, and photoluminescence spectra of the oligomers approximately fits the curve shown in SFigures 2 and 3. Here, the approximate relationship between absorption, excitation values, and the Hammett substituent[19] constants ($\sigma_p - R$) was maintained over the whole region of $\sigma_p - R$ values. These results revealed that the electronic effect of substituents on OPV3 provided an effective tool to tune the emissions of conjugated oligomers.

The photophysical properties of OPVs (a–g) together with radiative rate constant ($k_{rad}$), radiationless rate constant ($k_{nr}$), $k_{rad}/k_{nr}$ (a measure for emissivity), and emission lifetime ($\tau$) are summarized in Table 1. The lifetimes of the singlet excited state ($\tau$) were determined using single photon counting time-resolved photoluminescence. From the fluorescence quantum yields, $\tau$, $k_{rad}$, and $k_{nr}$ were calculated[20,21] (Table 1).

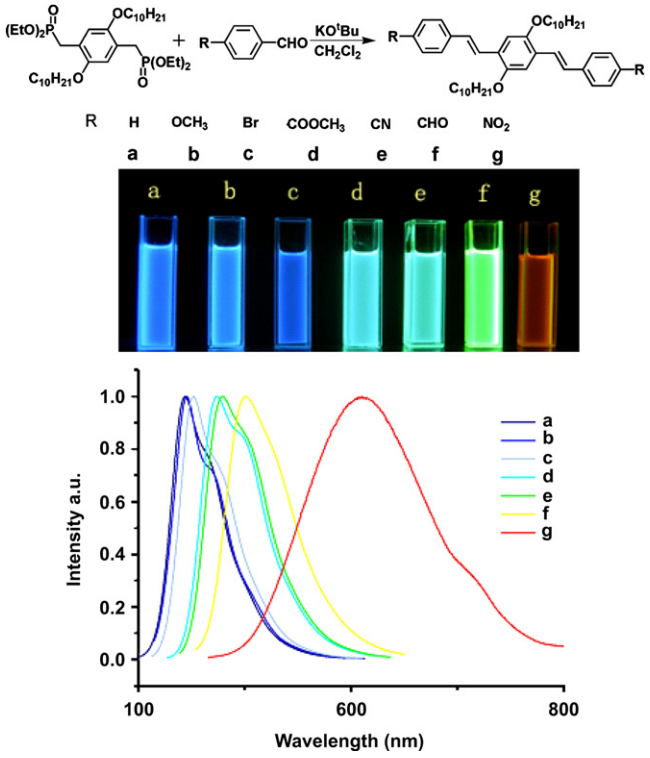


**Figure 1**. Molecular structure of the oligomers and normalized fluorescence spectra recorded in chloroform solutions of oligomers and emission photographs recorded in chloroform solutions with 365 nm excitation.

**Table 1**. Photophysical property of OPVs (a–g) (measured in $CHCl_3$)

| Compd | $\lambda_{ex}$ (nm) | $\lambda_{em}$ (nm) | $\Phi$[a] | $\lambda_{abs}$ (nm) | $\tau_F$ (ns) | $k_{rad}$ ($s^{-1}$) $10^{-8}$ | $k_{nr}$ ($s^{-1}$) $10^{-8}$ | $k_{rad}/k_{nr}$ |
|---|---|---|---|---|---|---|---|---|
| a | 389 | 444 | 0.65 | 389 | 2.0 | 3.3 | 1.8 | 1.86 |
| b | 392 | 446 | 0.09 | 392 | 1.46 | 0.62 | 6.2 | 0.10 |
| c | 393 | 452 | 0.48 | 397 | 1.18 | 4.1 | 4.4 | 0.92 |
| d | 407 | 474 | 0.96 | 411 | 1.58 | 6.1 | 0.25 | 24.0 |
| e | 413 | 479 | 0.85 | 415 | 1.64 | 5.2 | 0.91 | 5.67 |
| f | 424 | 502 | 0.68 | 423 | 1.75 | 3.9 | 1.8 | 2.13 |
| g | 440 | 610 | 0.08 | 446 | 0.745 | 1.1 | 12 | 0.09 |

[a] Quantum yield ($\Phi$) is measured using quinine sulfate in 0.1 M $H_2SO_4$, fluorescein in 1 M NaOH or rhodamine 6G as standards.

As shown in Table 1 and Figure 1, it was evident that the introduction of different groups at the side and end of rod-shaped OPVs changed the $\Phi$ and $\lambda_{em}$ values in comparison to those of the unsubstitutional OPV.[22,23] The emission maximum of the oligomers spanned over 166 nm between 444 and 610 nm, and the emission profiles covered almost the entire visible light spectra from blue and green to yellow and red. In particular, OPV3-g exhibited a large red-shift (108 nm) of the fluorescence emission maximum compared with OPV3-f and a significant decrease in the quantum yield due to a band gap decrease effected by the strong electron pulling effect of the nitryl group. However, it was already indicated by C. W. Tang that the fluorophore with nitryl group was not suitable for OLED applications.

The solvent dependency on the emissive characteristics of OPV3-e and g is shown in Table 2 and Figure 2. The $\Phi_f$ and $\lambda_{em}$ values of OPV3-g were remarkably altered with the change of solvent polarity. In contrast, little solvent dependency on $\Phi_f$ and $\lambda_{em}$ values of OPV3-e was observed. Solvent effect was also not apparently observed for the absorption spectra and excitation spectra of OPV3-e, whereas those of OPV3-g changed quite obviously in different polar solvents. The observed effect of the solvent polarity on the $\Phi_f$ values of OPV3-e and OPV3-g could be interpreted by the changes in their $k_{rad}$ and $k_{nr}$ values with changes in the solvent polarity. The $k_{rad}$ and $k_{nr}$ values of OPV3-e were not so altered by solvent polarity except in $CH_3OH$. On the contrary, those values were largely altered for OPV3-g with different solvent polarities. The contrary solvent polarity effect on $\Phi_f$, $\lambda_{em}$, $k_{rad}$, and $k_{nr}$ could be explained by a difference in the dipole moment of the excited state and of the ground state. The origin of this phenomenon is currently under investigation.

### 2.2. Electrochemistry

The redox properties of the oligomers were investigated by cyclic voltammetry (CV) in acetonitrile with $Bu_4NPF_6$ as supporting electrolyte. The results are summarized in Table 3. Oxidation and reduction potentials give information on the relative positions of the HOMO (highest occupied molecular orbital) and LUMO (lowest unoccupied molecular orbital). The band gaps for these compounds could be calculated from the first reduction and oxidation potentials as shown in Scheme 1. This was in good agreement with the determined band gap obtained from the onset of the absorbance shown in Table 3.

**Table 2**. Effect of solvent on photophysical property of OPV3-e and OPV3-g

| Compd | Solvent | $\lambda_{abs}$ (nm) | $\lambda_{em}$ (nm) | $\lambda_{ex}$ (nm) | $\Phi$ (%) | $\tau_F$ (ns) | $k_{nr}$ ($s^{-1}$) | $k_{rad}$ ($s^{-1}$) | $k_{nrad}/k_{nr}$ |
|---|---|---|---|---|---|---|---|---|---|
| e | Toluene | 413 | 470 | 416 | 71 | 2.34 | $1.24\times10^8$ | $3.03\times10^8$ | 2.44 |
| | $CHCl_3$ | 415 | 479 | 413 | 85 | 1.64 | $0.92\times10^8$ | $5.18\times10^8$ | 5.63 |
| | THF | 417 | 477 | 413 | 78 | 2.52 | $0.87\times10^8$ | $3.10\times10^8$ | 3.56 |
| | $CH_3CN$ | 409 | 492 | 415 | 76 | 2.39 | $1.0\times10^8$ | $3.18\times10^8$ | 3.18 |
| | $CH_3OH$ | 408 | 488 | 415 | 97 | 2.36 | $0.13\times10^8$ | $4.11\times10^8$ | 31.62 |
| g | Toluene | 434 | 507 | 442 | 45.7 | 1.92 | $2.82\times10^8$ | $2.38\times10^8$ | 0.84 |
| | $CHCl_3$ | 446 | 610 | 440 | 8.1 | 0.75 | $12.3\times10^8$ | $1.08\times10^8$ | 0.09 |
| | THF | 424 | 552 | 452 | 33.8 | 2.47 | $2.68\times10^8$ | $1.37\times10^8$ | 0.51 |
| | $CH_3CN$ | 437 | 598 | 432 | 0.06 | 1.80 | $5.56\times10^8$ | $3.3\times10^5$ | 6E-4 |
| | $CH_3OH$ | 437 | 500 | 439 | 0.15 | 2.27 | $4.4\times10^8$ | $6.6\times10^5$ | 1.5E-3 |

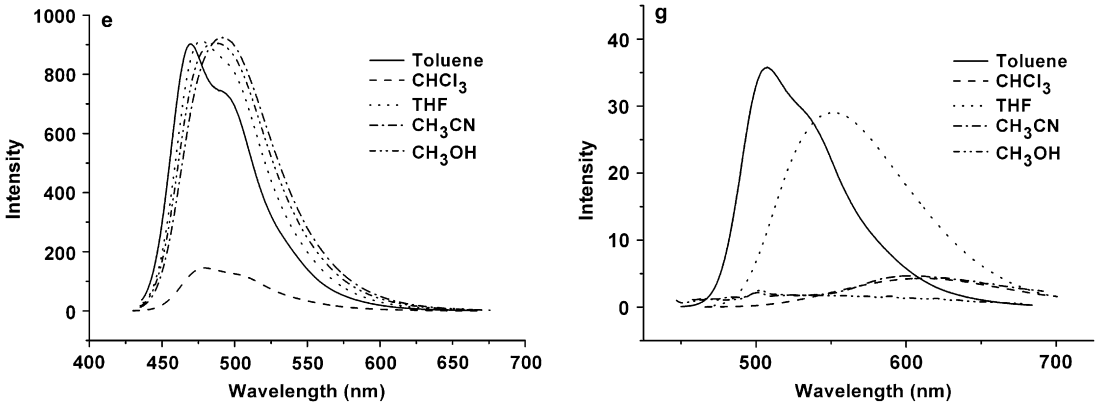


**Figure 2**. Fluorescence spectra of OPV3-e and OPV3-g recorded in different solvents ($6\times10^{-6}$ mol/L).

**Table 3**. Electrochemical data and physical measurement for the oligomers

| Compd | $E^3_{pa}$ | $E^2_{pa}$ | $E^1_{pa}$ | $E^{1b}_{pc}$ | $E^2_{pc}$ | $E^3_{pc}$ | HOMO (ev)[c] | LUMO (ev) | Band gap[a] (cv) (ev) | Band gap[b] (UV onset) (ev) |
|---|---|---|---|---|---|---|---|---|---|---|
| a | | 1.22 | 0.92 | −2.17 | −2.55 | | −5.31 | −2.22 | 3.09 | 3.17 (390) |
| b | 0.93 | 0.71 | 0.52 | −2.46 | | | −4.91 | −1.93 | 2.98 | 2.80 (443) |
| c | 1.32 | 1.12 | 0.95 | −2.05 | −2.19 | −2.55 | −5.34 | −2.34 | 3.0 | 2.80 (442) |
| d | | 1.29 | 1.02 | −1.87 | | | −5.41 | −2.52 | 2.89 | 2.63 (470) |
| e | | 0.87 | 0.73 | −1.84 | −2.12 | | −5.12 | −2.55 | 2.57 | 2.62 (473) |
| f | | 1.29 | 0.92 | −1.69 | −2.17 | −2.60 | −5.31 | −2.7 | 2.61 | 2.53 (490) |
| g | | | 1.087 | −1.35 | −1.86 | −2.43 | −5.47 | −3.04 | 2.43 | 2.33 (530) |

Cyclic voltammograms (CV) were performed in a solution of $Bu_4NPF_6$ (0.1 M) in acetonitrile using Glassy carbon electrode as working electrode, platinum wire as counter electrode, and Ag electrode as the reference electrode at a scan rate of 20 mV/s at room temperature under the protection of nitrogen. Ferrocene was used as an external standard, $E_{p(Fc/Fc+)}$=0.4 V versus Ag. pa=anodic peak. pc=cathodic peak.

[a] Energy gap was calculated from the redox potentials.

[b] Energy gap was estimated from the onset of absorption edge.

[c] LUMO=HOMO+energy gap.

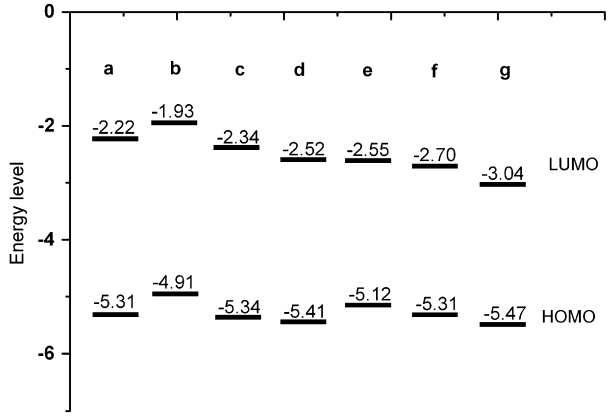


**Scheme 1**. Energy level of the oligomers calculated by electrochemical data.

In regard to structure–redox property relationship, it was found that the first redox potential value linearly increased with improved electron-accepting ability of end-substituent R as shown in Figure 3, where the linear relationship between the first redox potential and the Hammett substituent constants ($\sigma_p-R$) was maintained over the whole region of $\sigma_p-R$ values. The values of LUMO energy levels of the compounds were determined by comparing the first redox potential values. The similar linear relationship between the LUMO energy levels of the oligomers and the Hammett substituent constants ($\sigma_p-R$) is shown in Figure 3.

## 3. Conclusions

In conclusion, we succeeded in the creation of a series of new *p*-phenylenevinylene oligomer fluorophores. These

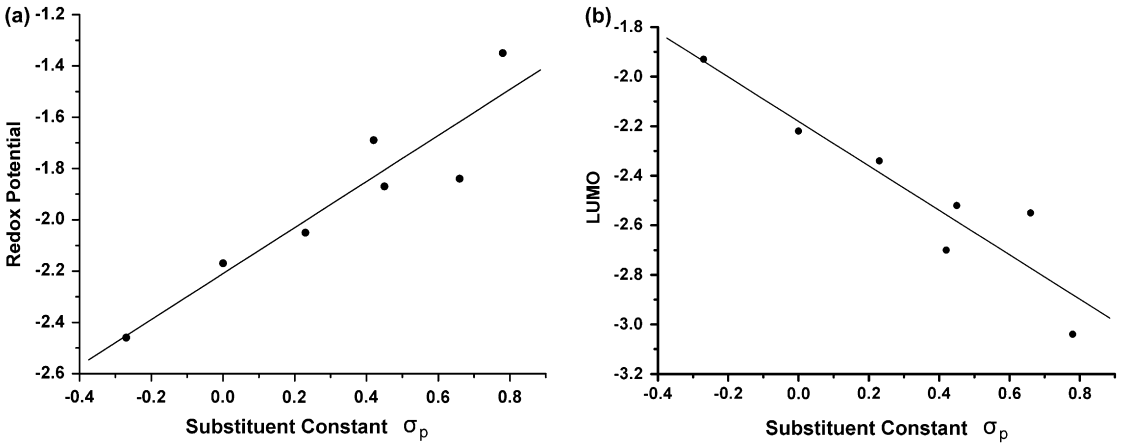


**Figure 3**. (a) A plot of the redox potential versus Hammett substituent constants $\sigma_p$; (b) a plot of LUMO energy level value versus Hammett substituent constants $\sigma_p$.

oligomers showed very intense blue (a, c), cyan (d, e), green (f), and red (g) emissions by the introduction of the appropriate end-substituent groups. The photophysical and electrochemical properties of the compounds were investigated by UV–vis, fluorescence spectroscopies, and cyclic voltammetry techniques. A successful tuning in the emission color was achieved and the LUMO energy level was found to correlate with the Hammett constant of the respective substituents, providing a powerful strategy for prediction of the photoelectric properties of new chromophores. In addition, contrary solvent dependency of photophysical properties of OPV3-e and OPV3-g, and a linear relationship between redox potential and $\sigma_p - R$ over the whole region were also found.

## 4. Experimental section

### 4.1. Materials and instruments

Most of the chemical reagents were purchased from Acros or Aldrich Corp. and were utilized as received unless indicated otherwise. All solvents were purified using standard procedures. Column chromatography was performed on silica gel (size 160–200 mesh). UV–vis spectra were taken on a Hitachi U-3010 spectrometer, and fluorescence spectra were measured on a Hitachi F-4500 spectrofluorometer. Cyclic voltammograms (CV) were recorded on CHI660B voltammetric analyzer (CH Instruments, USA). The CV were performed in a solution of $Bu_4NPF_6$ (0.04 M) in *o*-dichlorobenzene at a scan rate of 20 mV/s at room temperature under the protection of nitrogen. Glassy carbon electrode was used as the working electrode and Pt wire was used as the counter electrode. An Ag electrode was used as the reference electrode. The fluorescence lifetimes were measured on an Edinburgh Instruments Ltd FLS920. NMR spectra were obtained on a Bruker Avance DPS-400 (400 MHz) spectrometer. Mass spectra were obtained on Bruker BIFLEXIII spectrometer.

### 4.2. General procedure for the preparation of oligomers a–g

Diphosphonate and double amount of aldehyde-terminated aromatic ring were mixed in dry methylene chloride and purged with argon. Then potassium *tert*-butoxide (2 equiv, excess) was added, and the mixture was stirred for 2 h to complete the reaction. The cooled mixture was diluted with water. The precipitate was filtered and washed with methylene chloride. After concentration on a rotary evaporator, this solution was loaded onto a silica gel column and eluted with a mixture of petroleum and methylene chloride (1:1, v/v). This afforded oligomers as fluorescent solids.

**4.2.1. Compound a.** Yield: 78%. $^1$H NMR ($CDCl_3$, TMS): $\delta$ (ppm) 0.88 (s, 6H), 1.09–1.45 (m, 24H), 1.52–1.54 (m, 4H), 1.84–1.86 (m, 4H), 4.05 (s, 4H), 7.12–7.16 (m, 4H), 7.23–7.25 (m, 2H), 7.33–7.35 (m, 4H), 7.45 (s, 1H), 7.51–7.54 (m, 5H). $^{13}$C NMR ($CDCl_3$, TMS): $\delta$ 14.1, 22.7, 26.3, 29.3, 29.4, 29.5 29.6, 29.6, 31.9, 69.5, 110.6, 123.5, 126.5, 126.8, 127.3, 128.6, 128.7, 137.9, 151.1 ppm. MS *m/z*: 595 ($M^+$). Anal. Calcd for $C_{42}H_{58}O_2$: C, 84.79; H, 9.83. Found: C, 84.75; H, 9.86.

**4.2.2. Compound b.** Yield: 64%. $^1$H NMR ($CDCl_3$, TMS): $\delta$ (ppm) 0.88 (t, 6H, $J$=6.4 Hz), 1.25–1.27 (m, 24H), 1.52–1.55 (m, 4H), 1.85–1.88 (m, 4H), 3.83 (s, 6H), 4.04 (t, 4H, $J$=6.4 Hz), 6.89 (d, 4H, $J$=8.3 Hz), 7.05–7.09 (m, 4H), 7.31 (s, 1H), 7.35 (s, 1H), 7.46 (d, 4H, $J$=8.0 Hz). $^{13}$C NMR ($CDCl_3$, TMS): 14.0, 22.6, 26.2, 29.3, 29.4, 29.4, 29.5, 29.6, 31.8, 55.0, 69.3, 110.2, 121.2, 126.6, 127.6, 130.1, 130.7, 131.4, 131.5, 150.8, 150.9, 159.1 ppm. MS *m/z*: 655 ($M^+$). Anal. Calcd for $C_{44}H_{62}O_4$: C, 80.69; H, 9.54. Found: C, 80.72; H, 9.55.

**4.2.3. Compound c.** Yield: 56%. $^1$H NMR ($CDCl_3$, TMS): $\delta$ (ppm) 0.88 (t, 6H, $J$=6.4 Hz), 1.25–1.27 (m, 24H), 1.53–1.56 (m, 4H), 1.82–1.89 (m, 4H), 4.04 (t, 4H, $J$=6.4 Hz), 7.04 (s, 1H), 7.08 (s, 3H), 7.38 (d, 4H, $J$=8.0 Hz), 7.42 (s, 1H), 7.47 (d, 5H, $J$=7.7 Hz). $^{13}$C NMR ($CDCl_3$, TMS): 14.1, 22.7, 26.2, 29.3, 29.4, 29.5 29.6, 31.9, 53.4, 69.5, 110.5, 121.0, 124.1, 126.6, 127.6, 127.9, 131.7, 136.8, 151.0 ppm. MS *m/z*: 750 ($M^+$). Anal. Calcd for $C_{42}H_{56}Br_2O_2$: C, 67.02; H, 7.50. Found: C, 67.08; H, 7.46.

**4.2.4. Compound d.** Yield: 54%. $^1$H NMR ($CDCl_3$, TMS): $\delta$ (ppm) 0.88 (t, 6H, $J$=6.4 Hz), 1.23–1.28 (m, 24H), 1.50–1.56 (m, 4H), 1.84–1.89 (m, 4H), 4.05 (t, 4H, $J$=6.4 Hz), 4.36 (s, 6H), 7.11 (s, 2H), 7.14 (s, 1H), 7.19 (s, 1H), 7.55–7.59

(m, 6H), 8.03 (d, 4H, $J$=8.0 Hz). $^{13}$C NMR ($CDCl_3$, TMS): 13.9, 29.1, 29.1, 29.2 29.3, 29.4, 31.7, 51.8, 69.2, 110.5, 125.7, 126.0, 126.6, 127.7, 128.4, 129.8, 142.2, 151.0, 166.6 ppm. MS $m/z$: 711 ($M^+$). Anal. Calcd for $C_{46}H_{62}O_6$: C, 77.71; H, 8.79. Found: C, 77.65; H, 8.70.

**4.2.5. Compound e.** Yield: 58%. $^1$H NMR ($CDCl_3$, TMS): $\delta$ (ppm) 0.88 (t, 6H, $J$=6.6 Hz), 1.27–1.30 (m, 24H), 1.50–1.55 (m, 4H), 1.85–1.91 (m, 4H), 4.07 (t, 4H, $J$=6.4 Hz), 7.11–7.13 (m, 3H), 7.17 (s, 1H), 7.55 (s, 1H), 7.59 (d, 5H, $J$=8.0 Hz), 7.63 (d, 4H, $J$=8.4 Hz). $^{13}$C NMR ($CDCl_3$, TMS): 14.1, 22.6, 26.2, 29.3, 29.3, 29.5 29.6, 31.8, 69.4, 110.3, 110.7, 119.0, 126.7, 126.8, 127.0, 127.3, 132.4, 142.3, 151.3 ppm. MS $m/z$: 645 ($M^+$). Anal. Calcd for $C_{44}H_{56}N_2O_2$: C, 81.94; H, 8.75; N, 4.34. Found: C, 81.89; H, 8.80; N, 4.31.

**4.2.6. Compound f.** Yield: 68%. $^1$H NMR ($CDCl_3$, TMS): $\delta$ (ppm) 0.88 (t, 6H, $J$=6.4 Hz), 1.27–1.38 (m, 24H), 1.53–1.57 (m, 4H), 1.85–1.92 (m, 4H), 4.08 (t, 4H, $J$=6.4 Hz), 7.15 (s, 2H), 7.21 (s, 1H), 7.24 (s, 1H), 7.56 (s, 2H), 7.67 (d, 4H, $J$=9.6 Hz), 7.88 (d, 4H, $J$=10.8 Hz), 10.00 (s, 2H). $^{13}$C NMR ($CDCl_3$, TMS): 13.9, 22.4, 26.1, 29.1, 29.2, 29.3, 29.4, 31.6, 69.3, 110.6, 126.7, 127.7, 130.0, 135.0, 143.8, 151.2, 191.3 ppm. MS $m/z$: 651 ($M^+$). Anal. Calcd for $C_{44}H_{58}O_4$: C, 81.19; H, 8.98. Found: C, 81.22; H, 8.98.

**4.2.7. Compound g.** Yield: 57%. $^1$H NMR ($CDCl_3$, TMS): $\delta$ (ppm) 0.87 (t, 6H, $J$=6.4 Hz), 1.28–1.36 (m, 24H), 1.53–1.58 (m, 4H), 1.86–1.93 (m, 4H), 4.08 (t, 4H, $J$=6.4 Hz), 7.13 (s, 2H), 7.19 (s, 1H), 7.24 (s, 1H), 7.60–7.65 (m, 6H), 8.22 (d, 4H, $J$=8.0 Hz). $^{13}$C NMR ($CDCl_3$, TMS): 14.1, 22.7, 26.3, 29.3, 29.4, 29.4, 29.6, 29.7, 31.9, 69.5, 110.8, 124.2, 126.8, 127.0, 128.0, 144.4, 146.7, 151.5 ppm. MS $m/z$: 685 ($M^+$). Anal. Calcd for $C_{42}H_{56}N_2O_6$: C, 73.65; H, 8.24; N, 4.09. Found: C, 73.64; H, 8.18; N, 4.11.

## Acknowledgements

This work was supported by the National Natural Science Foundation of China and the Major State Basic Research Development Program (20531060, 10474101, 20418001, 20473102, and 20421101).

## Supplementary data

UV–vis spectra and substituent effect on absorption spectra, emission spectra, and excitation spectra of the oligomers. Supplementary data associated with this article can be found in the online version, at doi:10.1016/j.tet.2007.02.012.

## References and notes

1. Kraft, A.; Grimsdale, A. C.; Holmes, A. B. *Angew. Chem., Int. Ed.* **1998**, *37*, 402.
2. Friend, R. H.; Gymer, R. W.; Holmes, A. B.; Burroughes, J. H.; Marks, R. N.; Taliani, C.; Bradley, D. D. C.; Dos Santos, D. A.; Bre'das, J. L.; Lögdlund, M.; Salaneck, W. R. *Nature* **1999**, *397*, 121.
3. Mitschke, U.; Bäuerle, P. *J. Mater. Chem.* **2000**, *10*, 1471.
4. Chen, B. Z.; Wu, Y. Z.; Wang, M. Z.; Wang, S.; Sheng, S. H.; Zhu, W. H.; Sun, R. G.; Tian, H. *Eur. Polym. J.* **2004**, *40*, 1183.
5. (a) Katz, H. E. *J. Mater. Chem.* **1997**, *7*, 369; (b) Horowitz, G. *Adv. Mater.* **1998**, *10*, 365; (c) Garnier, F. *Acc. Chem. Res.* **1999**, *32*, 209.
6. Brabec, C. J.; Sariciftci, N. S.; Hummelen, J. C. *Adv. Funct. Mater.* **2001**, *11*, 15.
7. Hide, F.; Diaz-Garcia, M. A.; Schwartz, B. J.; Heeger, A. J. *Acc. Chem. Res.* **1997**, *30*, 430.
8. (a) Yamaguchi, Y.; Ochi, T.; Miyamura, S.; Tanaka, T.; Kobayashi, S.; Wakamiya, T.; Matsubara, Y.; Yoshida, Z.-i. *J. Am. Chem. Soc.* **2006**, *128*, 4504; (b) James, P. V.; Sudeep, P. K.; Suresh, C. H.; Thomas, K. G. *J. Phys. Chem. A* **2006**, *110*, 4329; (c) Yamaguchi, Y.; Tanaka, T.; Kobayashi, S.; Wakamiya, T.; Matsubara, Y.; Yoshida, Z.-i. *J. Am. Chem. Soc.* **2005**, *127*, 9332; (d) Yamaguchi, Y.; Ochi, T.; Wakamiya, T.; Matsubara, Y.; Yoshida, Z.-i. *Org. Lett.* **2006**, *8*, 717.
9. Robinson, M. R.; Wang, S.; Bazan, G. C.; Cao, Y. *Adv. Mater.* **2000**, *12*, 1701.
10. Oldham, W. J., Jr.; Lachicotte, R. J.; Bazan, G. C. *J. Am. Chem. Soc.* **1998**, *120*, 2987.
11. Yu, Y. H.; Mao, H. P.; Chen, L.; Lu, X. F.; Zhang, W. J.; Wei, Y. *Macromol. Rapid Commun.* **2004**, *25*, 664.
12. Tao, Y.; Donat-Bouillud, A.; D'Iorio, M.; Lam, J.; Gorjanc, T. C.; Py, C.; Wong, M. S.; Li, Z. H. *Thin Solid Films* **2000**, *363*, 298.
13. Tao, Y.; Donat-Bouillud, A.; D'Iorio, M.; Lam, J.; Gorjanc, T. C.; Py, C.; Wong, M. S. *Synth. Met.* **2000**, *111–112*, 417.
14. (a) Schenning, A.; Jonkheijm, P.; Peeters, E.; Meijer, E. W. *J. Am. Chem. Soc.* **2001**, *123*, 409; For reviews on self-assembled π-conjugated systems, see: (b) Hoeben, F. J. M.; Jonkheijm, P.; Meijer, E. W.; Schenning, A. *Chem. Rev.* **2005**, *105*, 1491; (c) Schenning, A.; Meijer, E. W. *Chem. Commun.* **2005**, 3245.
15. (a) Hoeben, F. J. M.; Herz, L. M.; Daniel, C.; Jonkheijm, P.; Schenning, A.; Silva, C.; Meskers, S. C. J.; Beljonne, D.; Phillips, R. T.; Friend, R. H.; Meijer, E. W. *Angew. Chem., Int. Ed.* **2004**, *43*, 1976; (b) Hoeben, F. J. M.; Schenning, A.; Meijer, E. W. *Chemphyschem* **2005**, *6*, 2337.
16. Tajima, K.; Li, L.; Stupp, S. I. *J. Am. Chem. Soc.* **2006**, *128*, 5488.
17. Müllen, K.; Wegner, G. *Electronic Materials: The Oligomer Approach*; Wiley-VCH: Weinheim, 1998; p 7.
18. Eckert, J.-F.; Nicoud, J.-F.; Nierengarten, J.-F.; Liu, S.-G.; Echegoyen, L.; Barigelletti, F.; Armaroli, N.; Ouali, L.; Krasnikov, V.; Hadziioannou, G. *J. Am. Chem. Soc.* **2000**, *122*, 7467.
19. Yeh, S. J.; Chen, H. Y.; Wu, M. F.; Chan, L. H.; Chiang, C. L.; Yeh, H. C.; Chen, C. T.; Lee, J. H. *Org. Electron.* **2006**, *7*, 137.
20. Wang, J.; Yu, G.; Srdanov, G.; Heeger, A. J. *Org. Electron.* **2000**, *1*, 33.
21. Values for $k_{rad}$ and $k_{nr}$ were obtained by using data in Table 1 and the following equations: $k_{rad}=\Phi/\tau_F$ and $k_{nr}=1/\tau_F-k_{rad}$.
22. Oelkrug, D.; Tompert, A.; Gierschner, J.; Egelhaaf, H.-J.; Hanack, M.; Hohloch, M.; Steinhuber, E. *J. Phys. Chem. B* **1998**, *102*, 1902.
23. Egelhaaf, H. J.; Gierschner, J.; Oelkrug, D. *Synth. Met.* **1996**, *83*, 221.